



Published in final edited form as:

Int J Radiat Oncol Biol Phys. 2022 March 15; 112(4): 1055–1062. doi:10.1016/j.ijrobp.2021.11.008.

Mathematical Modeling to Simulate the Effect of Adding Radiation Therapy to Immunotherapy and Application to Hepatocellular Carcinoma

Wonmo Sung, PhD^{*,†}, Theodore S. Hong, MD[‡], Mark C. Poznansky, MD, PhD^{§,||}, Harald Paganetti, PhD^{*}, Clemens Grassberger, PhD^{*}

^{*}Division of Biophysics, Department of Radiation Oncology, Massachusetts General Hospital, Boston, Massachusetts

[†]Department of Biomedical Engineering and Department of Biomedicine and Health Sciences, College of Medicine, The Catholic University of Korea, Seoul, South Korea

[‡]Department of Radiation Oncology, Massachusetts General Hospital, Boston, Massachusetts

[§]Department of Medicine, Massachusetts General Hospital, Boston, Massachusetts

^{||}Vaccine and Immunotherapy Center, Massachusetts General Hospital, Boston, Massachusetts

Abstract

Purpose: To develop a comprehensive framework to simulate the response to immune checkpoint inhibitors (ICIs) in combination with radiation therapy (RT) and to apply the framework for investigating ICI-RT combination regimen in patients with hepatocellular carcinoma (HCC).

Methods and Materials: The mechanistic mathematical model is based on dynamic biological interactions between the immune system and the tumor using input data from patient blood samples and outcomes of clinical trials. The cell compartments are described by ordinary differential equations and represent irradiated and nonirradiated tumor cells and lymphocytes. The effect of ICI is modeled using an immune activation term that is based on tumor size changes observed in a phase 1/2 clinical trial for HCC. Simulated combination regimen are based on ongoing ICI-RT trials.

Results: The proposed framework successfully describes tumor volume trajectories observed in early-stage clinical trials of durvalumab monotherapy in patients with HCC. For ICI-RT treatment regimen the irradiated tumor fraction is the most important parameter for the efficacy. For 90% of the tumor cells being irradiated, adding RT to ICI yields an increase in clinical benefit from 33% to 71% in nonirradiated tumor sites. The model agrees with clinical data showing an association

Corresponding author: Clemens Grassberger, PhD; Grassberger.Clemens@mgh.harvard.edu.

Disclosures: H.P. has research collaborations with Raysearch Laboratories (Stockholm, Sweden) and GE Global Research (Niskayuna, New York). T.S.H. serves on advisory boards with EMD Serono and Merck and has research collaborations with Taiho Astra-Zeneca, BMS, IntraOp, Novartis, and Tesaro. C.G. serves on the scientific advisory board of Nanolive SA.

Research data are stored in an institutional repository and will be shared upon request to the corresponding author.

Supplementary material associated with this article can be found, in the online version, at doi:10.1016/j.ijrobp.2021.11.008.

of outcome with initial tumor volume and lymphocyte counts. We demonstrate model application in clinical trial design to predict progression-free survival curves, showing that the cohort size to show significant improvement heavily depends on the irradiated tumor fraction.

Conclusions: We present a framework extending radiation cell kill models to include circulating lymphocytes and the effect of ICIs and enable simulation of combination strategies. The simulations predict that a significant amount of the benefit from RT in combination with ICI stems from the reduction in irradiated tumor burden and associated immune suppression. This aspect needs to be included in the interpretation of outcomes and the design of novel combination trials.

Introduction

The role of radiation in cancer treatment is expanding. Traditionally radiation therapy (RT) has been considered a local treatment, damaging DNA directly to eradicate tumor cells. However, there is growing evidence showing that radiation also possesses immunostimulatory characteristics.¹ As such, radiation is currently being investigated as a treatment option for metastatic disease in conjunction with systemic agents, particularly immune checkpoint inhibitors (ICIs). ICIs block checkpoint proteins that inhibit the efficacy of antitumor effector T cells from binding with their partner proteins and thereby prevent cancer cells from evading the immune system, allowing T cells to attack the tumor.² Adding RT to ICI is thought to improve clinical efficacy and is investigated across multiple indications, including hepatocellular carcinoma (HCC).^{2,3}

Despite the growing number of trials combining RT and ICI and general enthusiasm, there have been positive⁴ as well as negative results,⁵ and concerns persist that this approach might be limited by radiation-induced immunosuppression due to the high radiosensitivity of lymphocytes. Additionally, the appropriate choice of RT regimen in combination with ICI is an open question because preclinical data has shown that efficacy can depend on dose,⁶ sequencing,⁷ timing,⁸ and fractionation.^{6,7} Preclinical data are scarce regarding the choice of combination regimen, and, though many clinical trials are ongoing to test ICI-RT combinations, it is impractical to conduct all of the possible combinations in separate trial arms. Nonetheless, there are no mathematical approaches to model the effects of ICI and RT on the combined tumor-immune system. Previous studies were focused either on ICI treatments, mainly with the purpose to find early indicators of response^{9,10} or to simulate the lymphocyte depletion of RT alone,^{11,12} and were often tailored to animal experiments.^{13–15} To our knowledge, the present study is the first approach to formalize a model to design a combination trial based on RT and ICI patient data.

The purpose of this study is threefold: (1) to extend an existing RT outcome modeling framework to include the effects of immune checkpoint inhibition; (2) to demonstrate the ability to parameterize this framework based on reported response rates for ICI monotherapy in patients; (3) to investigate the possible efficacy of recently initiated ICI-RT combination trials, focusing on the possible effects of extent of irradiation, sequencing, and fractionation.

Methods and Materials

The tumor-immune-radiation model

The tumor-immune radiation model is an extension of a previously published model focusing on the effect of RT only, which is fitted to local control, distant progression, and lymphocyte depletion in patients with HCC during and after RT.¹¹ Similar to the original model, in our model we simulate the dynamic relationships between tumor growth, circulating lymphocytes, and treatment effect using 4 compartments: (1) irradiated tumor cells T_I , (2) nonirradiated tumor cells T_{NI} , (3) inactivated tumor cells I , (4) circulating lymphocytes L . Figure 1 shows a schematic overview of the model and the main interactions together with the differential equations describing the model (also detailed in Section E1 in the supplementary material). Table 1 lists the model parameters. We include the effects of exponential tumor growth, immune-mediated tumor cell kill, linear-quadratic radiation tumor cell kill, and circulating immune cells. Both tumor compartments are affected by immune-induced cell death, but only the irradiated one experiences cell kill by RT, leading to inactivated tumors cells (I). The model assumes that the number of tumor-directed effector lymphocytes (L) increases with tumor antigen presentation, which is proportional to the cells inactivated by RT, and is decaying constantly otherwise. We use an empirical Monod form ($T/(g + T)$) (also called Michaelis-Menten term) with a half-saturation constant g . This form accounts for the saturation effects due to a reduced fraction of the increasing tumor volume being in contact with circulating lymphocytes as described by Kirschner and Panetta.¹⁶ Additionally, lymphocytes are also killed by radiation, which is calculated using a dynamic blood dose-volume histogram model specific to liver irradiation¹⁷ (see supplementary material Sections E1 and E2). The blood irradiation model considers the effects of fractionation on lymphocyte depletion.¹⁷

One of the distinct features of our model is the separation of irradiated and nonirradiated tumor compartments. The number of irradiated tumor cells is affected by both local and systemic therapy, whereas the number of nonirradiated tumor cells is targeted only by systemic therapy. We focus on RT as local treatment and ICI as a systemic agent in this study. Thus, the nonirradiated tumor is typically metastasized tumor, which is not within the radiation field. We separate the compartments to simulate their differential dynamics due to the different therapies affecting them and because their sizes are observables that can be estimated for specific patients.

Compared with our previously developed and parameterized RT-only model,¹¹ the new formalism has one additional term (Fig. 1, shown in red): this term increases ω_I , which determines the effector-lymphocyte coupling strength and thereby simulates the increase in cell kill by effector lymphocytes induced by immune checkpoint inhibition. Except for the new term, all parameters have been deduced in the RT-only model.¹¹ As shown in Figure E1, these parameters are fixed to derive the one remaining parameter to describe ICI response (δ_{durva}). Table 1 summarizes the resulting population average parameters, their standard deviations, and their source.

Model fit to immunotherapy response data

To investigate ICI-RT combination regimen using our modeling framework, we needed to ensure our model correctly describes the effects of these 2 modalities separately. For RT, this has been previously demonstrated.¹¹ The ICI-related parameter is separately fitted to clinical trial data of patients with HCC receiving durvalumab monotherapy.^{18,19}

Patient response is classified based on RECIST 1.1 criteria (Table E1) into 4 categories: (1) complete response (CR), (2) partial response (PR), (3) stable disease (SD), and (4) progressive disease (PD), as in two current clinical trials.^{18,19} The maximum concentration (C_{max}) and the biological half-life of durvalumab ($t_{1/2}$) are known from pharmacodynamic studies,²⁰ so that only δ_{durva} can be fitted to the trial data. It represents the increase in cell kill by effector lymphocytes induced by the immune checkpoint inhibitor. To represent the variability in patient response to ICIs, we assume δ_{durva} is normally distributed in the population and can be characterized by a mean and standard deviation, which is fitted to the observed clinical outcomes similar to our previous work.¹¹ We also assume a diameter of 6 mm as the minimal observable lesion using current diagnostic techniques.²¹ Comorbidity related deaths are implemented using a Monte Carlo method, simulating a rate of 3.6% fatal adverse events per month according to reported outcomes in patients with HCC.²²

To estimate the distributions of δ_{durva} , we first generate groups of 10,000 patients with fixed δ_{durva} values (0–0.5) and predict their responses by measuring tumor size at 2 years, see supplementary Figure 2 for the response rate as a function of δ_{durva} . As δ_{durva} increases, the SD, PR and CR rates rise and then decrease sequentially. SD and PR rates peak because when δ_{durva} increases, the response of those patients improving from SD to PR and from PR to CR respectively. Based on Figure E2, we can estimate a unique δ_{durva} distribution that fits the observed clinical response in the durvalumab monotherapy trial¹⁸: CR = 0%, PR = 10%, and SD = 22.5%. The estimated average and standard deviation of the resulting δ_{durva} distribution are 0.12 and 0.04 (see Section E2 for details), respectively, and these values are used in all ICI-RT combination simulations. Supplementary Figure E3 shows the distributions of the initial tumor size ($T_0 = T_{I, initial} + T_{NI, initial}$), circulating lymphocyte (L_0), tumor radiation sensitivity (α_T), and ICI effectiveness (δ_{durva}).

Results

Simulating ICI-RT combination regimen

The simulated ICI-RT combination regimen is based on the treatment protocol of an ongoing clinical trial.²³ Accordingly, RT consists of 8 Gy on 3 consecutive days, delivered concurrently with the second cycle of the ICI treatment (2 weeks after the first dose). We explore possible changes in outcome for different RT parameters: irradiated tumor fraction (ITF, the fraction of visible tumor burden that is targeted with RT), treatment sequence, initial tumor volume, baseline lymphocyte counts, total dose, and fractionation (for an overview of parameter combinations, see Table E2).

Irradiated tumor fraction

Figure 2 shows simulation results for adding 24 Gy delivered in 3 fractions to ICI in a simulated population of patients with HCC (Fig. E4). The left panel shows the results quantified using RECIST1.1 as a function of irradiated tumor fraction, and the right shows waterfall plots of the responses of an example cohort of 100 patients with 2 different irradiated tumor fractions (ITF is 10% on left and 90% on right). The response when irradiating a small tumor burden are identical to ICI only, with 23% stable disease and 10% partial response. When irradiating a larger fraction of the tumor, however, response rates start to increase and reach 29% stable disease, 34% partial response, and 9% complete response when irradiating 90% of visible tumor burden. The clinical benefit (sum of SD, PR and CR) increases from 33% to 72% when increasing the irradiated tumor fraction.

Sequencing

Next, we investigate the effects of the timing of RT with regard to the start of ICI administration (Fig. 3). As shown in Figure 3A, negative values denote RT starting before ICI and positive values mean RT starts after initiation of ICI. Figure 3B shows the simulated response rate for nonirradiated tumor. The response is maximal when RT and ICI start concurrently, but the asymmetrical fall-off regarding RT administration before versus after ICI start was unexpected and is further discussed below (see also Fig. E5).

Other treatment factors

Figures E6, E7, and E8 show the simulation results for initial tumor volume, initial absolute lymphocyte counts, total dose and fractionation. An increased baseline tumor burden lowers the response rate to ICI monotherapy, though the addition of RT can lessen this effect of larger tumor burdens considerably (Fig. E6). The effect of the patient's initial lymphocyte counts is not significant for RT alone, but increases for ICI monotherapy and ICI-RT combination therapies (Fig. E7), which has been observed in patients and is further discussed below. For dose and fractionation, we have simulated a number of scenarios that would be clinically feasible: in addition to the baseline scenario of 8 Gy \times 3 currently evaluated in a clinical trial (NCT03482102),²³ we have simulated 8 Gy \times 1, 8 Gy \times 2, and 2 15-fraction regimen that are currently used for definitive RT in HCC (3.87/4.5Gy \times 15). The simulations indicate that, whereas for the lowest dose level (8Gy \times 1) the efficacy of the ICI-RT combination regimen is reduced, the response rates in nonirradiated tumor are similar for 16 Gy/2fx, 24 Gy/3fx, 58.05 Gy/15fx, and 67.5 Gy/15fx (Fig. E8B). Similarly, changing the fractionation while keeping the biologically effective dose to the tumor constant does not affect response rates (Fig. E8A). These simulations neglect the differential effects that have been observed for large fraction sizes regarding immune activation in preclinical experiments,^{6,24} as further discussed below.

Mathematical model for clinical trial design

Because our framework builds on parameter distributions that were fitted to population outcomes, it accurately reflects the heterogeneity in treatment response to ICI as well as RT in the underlying population. Therefore, the model does not only provide predictions of the

expected outcome, but it can also be used to estimate the number of required patients to show these simulated effects in clinical trials.

This is demonstrated in Figure 4A, which shows the predicted progression-free survival of 32 patients treated with ICI monotherapy, the observed outcomes in the ICI monotherapy trial (green dots)¹⁹ and 2 ICI-RT combination regimen, one assuming that the irradiated tumor fraction is 50%, the other assuming 90%. To separate the local effect of RT from its synergy with ICI in nonirradiated lesions, Figure 4 is showing progression in nonirradiated lesions only. Using repeated random sampling from our population distributions we calculated a median outcome and the 95% confidence interval. This figure is the equivalent of Figure 2 for ITF of 50% and 90%, but instead of displaying the RECIST response rates we show the entire progression-free survival curve for each arm, for both a small cohort ($n = 32$ patients in each arm) (Fig. 4A) and a large cohort ($n = 256$ patients in each arm) (Fig. 4B). What Figure 4 clearly demonstrates is that for a small pilot trial of ICI-RT versus ICI, the outcomes with an ITF of 50% would not be statistically significant from each other ($P = 0.25 \pm 0.23$ over 100 iterations in Figure 4A), whereas when irradiating 90% of visible tumor burden (ITF = 90%) the likelihood of observing statistical significance is high (P value = 0.02 ± 0.05 over 100 iterations).

Discussion

Clinical trials are essential to test the efficacy of new cancer treatments and provide the foundation for evidence-based clinical decision-making. For a wide variety of indications, successful cancer therapy is not based on a single treatment modality, but rather on combination strategies. Especially in the case of drug-radiation trials this creates additional challenges, as there are a multitude of RT treatment parameters that can be adjusted and could affect the efficacy of the overall treatment (sequencing, dose, fractionation, patient selection). Because incorporating different combination arms is costly and time consuming, mathematical modeling can be used to conduct in-silico virtual clinical trials that can guide the design of the actual treatment arms. This is particularly useful in the context of ICI-RT combinations, where current clinical trials use a wide variety of different RT regimen.^{2,19}

To address this challenge, we propose a tumor-immune-radiation framework that integrates the therapeutic effects of immune checkpoint inhibition, RT and their possible synergy. The previous framework describing the immune cell dynamics during and after RT is extended in this current study to include the effect of immune checkpoint inhibition by modifying the immune related tumor cell kill term to include their effects (Figure 1, shown in red). We design this framework with 2 principles in mind: (1) one should be able to parameterize it only based on observables and patient outcomes; (2) it should take into account the underlying heterogeneity of the patient population. To achieve the former we restricted the simulated compartments to observables (tumor burden, lymphocyte count) and parameters that can be reasonably estimated in patients (tumor growth, radiation sensitivity, number of lethally irradiated tumor cells). The ultimate purpose of this model is not to capture all relevant underlying biological mechanisms, but it focuses on the RT parameters that we can control (sequencing, irradiated tumor fraction, dose, and fractionation) to guide clinical trial design or adaptation of treatment for specific subgroups. Furthermore, we

have purposefully not included a term to simulate direct radiation-induced enhancement of the immune response, but only the indirect enhancement via tumor load reduction. Future clinical data will indicate if such a term is required and will allow us to parameterize it. Such a direct stimulation effect can be added either by increasing the effector-lymphocyte coupling strength, adding a term to the third equation (Fig. 1B), or by increasing the number of infiltrating effector lymphocytes, which represents 2 different ways in which radiation has been shown to stimulate immune responses.

We parameterized our model based on clinical data of patients with HCC treated only with RT²⁵ or immune checkpoint inhibition¹⁹ and apply it to predict the outcome of currently ongoing ICI-RT combination trials.²³ Our framework predicts several behaviors that have been clinically observed. Figure 3 shows the effect of sequencing and timing for treatment efficacy. Responses were maximized if ICI and RT are delivered at the same time, decreasing significantly when there is a gap, for example, when larger breaks occur after the end of RT and start of adjuvant ICI. These results are in accordance with analyses of the PACIFIC study for adjuvant durvalumab after chemo-radiation, which showed improved outcome when adjuvant ICI was started earlier within 14 days as opposed to 14 days after starting RT.²⁶ Furthermore, the framework correctly reproduces the prognostic value of baseline absolute lymphocyte counts for ICI efficacy²⁷ and the observations that patients with larger tumor burden generally have lower response to immunotherapy, a phenomenon observed across multiple indications.^{28–30} The simulations also predict that the correlation of baseline lymphocyte count with outcome is stronger for ICI-RT combinations than after RT alone, which has recently been reported in non-small cell lung cancer treated with adjuvant ICI compared with chemoradiation only.^{31,32}

Most important, we found that the fraction of irradiated tumor burden has significant effect on the efficacy of combined ICI-RT regimen. The benefits of adding ICI to RT is increasingly improved in patients where less disease was left untreated. This needs to be taken into account when analyzing outcomes of ICI-RT combination regimen because this factor can vary among patients and trials. Studies have shown that irradiating small fractions of the tumor burden can lead to little synergy,⁵ and it has been proposed that RT to a larger extent of tumor can increase efficacy.³³

Although the model is able to include the effects of ICI and RT, future observations in combination trials might require modifications or extensions to accommodate observed outcomes. Currently the framework has the following limitations: (a) No explicit mechanisms are included to make the antigen-releasing effect of RT fraction-size dependent, as was shown in preclinical studies,⁶ though not yet in patients. Also, as discussed above, although our current model includes direct immunosuppressive mechanisms of RT, it does not include possible direct enhancement effects of RT that have been observed in preclinical studies.² (b) Currently the tumor is modeled as one compartment, without consideration of different patterns of spread (singular distant brain metastasis versus widely disseminated disease). (c) The lymphocyte compartment we are simulating is the “absolute” lymphocyte count because we had multiple measurements before, throughout, and after RT to parameterize our model.¹¹ (d) Normal tissue toxicity is not considered for RT and ICI. Especially renal adverse events caused by ICI therapy pose a unique challenge to

clinicians. The underlying assumption in this work is that the proposed RT and ICI regimen do not alter the toxicity profile of the treatment to an extent that has an effect on survival events. Suggestions for future extensions are further described in Section E6. As shown in successful translations of model-derived treatment protocols, prospective clinical trials to evaluate and improve the quantitative accuracy of the current model are required.^{34–36} Ultimately, although our model describes the small amount of available data, only more clinical data on combination regimen will be able to answer the question how well our model equations describe actual dynamics and outcomes and if certain terms have to be modified.

Conclusions

We propose a framework that integrates the effect of immune checkpoint inhibition and RT, and their possible synergy through tumor burden reduction and antigen release. We fit the model independently to single-modality ICI and RT patient outcomes and simulate currently investigated combination regimen. The model reproduces several relationships observed in clinical data, and for the first time provides a framework that could enable optimization of RT together with immune checkpoint inhibitors. Our simulations suggest that for ICI-RT combination approaches in metastatic patients, the fraction of irradiated tumor burden has a large effect on treatment efficacy and has to be included when analyzing treatment efficacy. The framework captures heterogeneity among patients regarding tumor mass, lymphocyte counts, and sensitivity to RT and ICI, and could be used to guide patient selection and clinical trial design to maximize efficacy of ICI-RT combination regimen.

Supplementary Material

Refer to Web version on PubMed Central for supplementary material.

Acknowledgments

This work was supported by grants from the National Institutes of Health (R21 CA241918, PI: Grassberger) and a grant from the National Research Foundation of Korea (NRF) funded by the Korea government (MEST) (No. 2021R1C1C1005930), and through financial support from the Catholic Medical Center Research Foundation (made in the program year of 2020).

References

1. Antonia SJ, Villegas A, Daniel D, et al. Durvalumab after chemoradiotherapy in stage III non-small-cell lung cancer. *N Engl J Med* 2017;377:1919–1929. [PubMed: 28885881]
2. Grassberger C, Ellsworth SG, Wilks MQ, Keane FK, Loeffler JS. Assessing the interactions between radiotherapy and antitumor immunity. *Nat Rev Clin Oncol* 2019;16:729–745. [PubMed: 31243334]
3. Choi C, Yoo GS, Cho WK, Park HC. Optimizing radiotherapy with immune checkpoint blockade in hepatocellular carcinoma. *World J Gastroenterol* 2019;25:2416–2429. [PubMed: 31171886]
4. Formenti SC, Rudqvist NP, Golden E, et al. Radiotherapy induces responses of lung cancer to CTLA-4 blockade. *Nat Med* 2018;24:1845–1851. [PubMed: 30397353]
5. McBride S, Sherman E, Tsai CJ, et al. Randomized phase II trial of nivolumab with stereotactic body radiotherapy versus nivolumab alone in metastatic head and neck squamous cell carcinoma. *J Clin Oncol* 2021;39:30–37. [PubMed: 32822275]

6. Vanpouille-Box C, Alard A, Aryankalayil MJ, et al. DNA exonuclease Trex1 regulates radiotherapy-induced tumour immunogenicity. *Nat Commun* 2017;8:15618. [PubMed: 28598415]
7. Young KH, Baird JR, Savage T, et al. Optimizing timing of immunotherapy improves control of tumors by hypofractionated radiation therapy. *PLoS One* 2016;11 e0157164. [PubMed: 27281029]
8. Lai X, Stiff A, Duggan M, Wesolowski R, Carson WE 3rd, Friedman A. Modeling combination therapy for breast cancer with BET and immune checkpoint inhibitors. *Proc Natl Acad Sci U S A* 2018;115:5534–5539. [PubMed: 29735668]
9. Butner JD, Elganainy D, Wang CX, et al. Mathematical prediction of clinical outcomes in advanced cancer patients treated with checkpoint inhibitor immunotherapy. *Sci Adv* 2020;6:eaay6298. [PubMed: 32426472]
10. Butner JD, Wang Z, Elganainy D, et al. A mathematical model for the quantification of a patient's sensitivity to checkpoint inhibitors and long-term tumour burden. *Nat Biomed Eng* 2021;5:297–308. [PubMed: 33398132]
11. Sung W, Grassberger C, McNamara AL, et al. A tumor-immune interaction model for hepatocellular carcinoma based on measured lymphocyte counts in patients undergoing radiotherapy. *Radiother Oncol* 2020;151:73–81. [PubMed: 32679308]
12. Jin JY, Mereniuk T, Yalamanchali A, et al. A framework for modeling radiation induced lymphopenia in radiotherapy. *Radiother Oncol* 2020;144:105–113. [PubMed: 31794944]
13. Rodriguez-Perez D, Sotolongo-Grau O, Espinosa Riquelme R, et al. Assessment of cancer immunotherapy outcome in terms of the immune response time features. *Math Med Biol* 2007;24:287–300. [PubMed: 17652107]
14. Poleszczuk J, Enderling H. The optimal radiation dose to induce robust systemic anti-tumor immunity. *Int J Mol Sci* 2018;19:3377.
15. Serre R, Benzekry S, Padovani L, et al. Mathematical modeling of cancer immunotherapy and its synergy with radiotherapy. *Cancer Res* 2016;76:4931–4940. [PubMed: 27302167]
16. Kirschner D, Panetta JC. Modeling immunotherapy of the tumor-immune interaction. *J Math Biol* 1998;37:235–252. [PubMed: 9785481]
17. Basler L, Andratschke N, Ehrbar S, Guckenberger M, Tanadini-Lang S. Modelling the immunosuppressive effect of liver SBRT by simulating the dose to circulating lymphocytes: An in-silico planning study. *Radiat Oncol* 2018;13:10. [PubMed: 29357886]
18. U.S. National Library of Medicine. Hwu W-J. A phase 1/2 study to evaluate the safety, tolerability, and pharmacokinetics of MEDI4736 in subjects with advanced solid tumors. Available at: <https://clinicaltrials.gov/ct2/show/NCT01693562>. Accessed December 13, 2021.
19. Wainberg ZA, Segal NH, Jaeger D, et al. Safety and clinical activity of durvalumab monotherapy in patients with hepatocellular carcinoma (HCC). *J Clin Oncol* 2017;35(15_suppl):4071.
20. Baverel PG, Dubois VFS, Jin CY, et al. Population pharmacokinetics of durvalumab in cancer patients and association with longitudinal biomarkers of disease status. *Clin Pharmacol Ther* 2018;103:631–642. [PubMed: 29243223]
21. Hwang J, Kim SH, Lee MW, Lee JY. Small (< 2 cm) hepatocellular carcinoma in patients with chronic liver disease: Comparison of gadoxetic acid-enhanced 3.0 T MRI and multiphase 64-multirow detector CT. *Br J Radiol* 2012;85:e314–e322. [PubMed: 22167508]
22. Sanford NN, Pursley J, Noe B, et al. Protons versus photons for unresectable hepatocellular carcinoma: Liver decompensation and overall survival. *Int J Radiat Oncol Biol Phys* 2019;105:64–72. [PubMed: 30684667]
23. U.S. National Library of Medicine. Hong TS. A phase II trial of durvalumab (MEDI4736) and tremelimumab and radiation therapy in hepatocellular carcinoma and biliary tract cancer. Available at: <https://clinicaltrials.gov/ct2/show/NCT03482102>. Accessed December 13, 2021.
24. Dewan MZ, Galloway AE, Kawashima N, et al. Fractionated but not single-dose radiotherapy induces an immune-mediated abscopal effect when combined with anti-CTLA-4 antibody. *Clin Cancer Res* 2009;15:5379–5388. [PubMed: 19706802]
25. Hong TS, Wo JY, Yeap BY, et al. Multi-institutional phase II study of high-dose hypofractionated proton beam therapy in patients with localized, unresectable hepatocellular carcinoma and intrahepatic cholangiocarcinoma. *J Clin Oncol* 2016;34:460–468. [PubMed: 26668346]

26. Bang A, Schoenfeld JD, Sun AY. Pacific: Shifting tides in the treatment of locally advanced non-small cell lung cancer. *Transl Lung Cancer Res* 2019;8:S139–S146. [PubMed: 31673518]
27. Diehl A, Yarchoan M, Hopkins A, Jaffee E, Grossman SA. Relationships between lymphocyte counts and treatment-related toxicities and clinical responses in patients with solid tumors treated with PD-1 checkpoint inhibitors. *Oncotarget* 2017;8 114268. [PubMed: 29371985]
28. Cho Y, Park S, Byun HK, et al. Impact of treatment-related lymphopenia on immunotherapy for advanced non-small cell lung cancer. *Int J Radiat Oncol Biol Phys* 2019;105:1065–1073. [PubMed: 31476418]
29. Joseph RW, Elassaiss-Schaap J, Kefford R, et al. Baseline tumor size is an independent prognostic factor for overall survival in patients with melanoma treated with pembrolizumab. *Clin Cancer Res* 2018;24:4960–4967. [PubMed: 29685882]
30. Massa RC, Sparrow M, Lin H, et al. Relationship between pre-treatment organ-specific tumor burden (TB) and response to immunotherapy in advanced melanoma (MEL). *J Clin Oncol* 2018;36(suppl): e21507. 15–e21507.
31. Tang C, Liao Z, Gomez D, et al. Lymphopenia association with gross tumor volume and lung V5 and its effects on non-small cell lung cancer patient outcomes. *Int J Radiat Oncol Biol Phys* 2014;89:1084–1091. [PubMed: 25035212]
32. Friedes C, Chakrabarti T, Olson S, et al. Association of severe lymphopenia and disease progression in unresectable locally advanced non-small cell lung cancer treated with definitive chemoradiation and immunotherapy. *Lung Cancer* 2021;154:36–43. [PubMed: 33611224]
33. Brooks ED, Chang JY. Time to abandon single-site irradiation for inducing abscopal effects. *Nat Rev Clin Oncol* 2019;16:123–135. [PubMed: 30401936]
34. Leder K, Pitter K, LaPlant Q, et al. Mathematical modeling of PDGF-driven glioblastoma reveals optimized radiation dosing schedules. *Cell* 2014;156:603–616. [PubMed: 24485463]
35. Alfonso Lopez J C, Parsai S, Joshi N, et al. Temporally feathered intensity-modulated radiation therapy: A planning technique to reduce normal tissue toxicity. *Med Phys* 2018;45:3466–3474. [PubMed: 29786861]
36. Prokopiou S, Moros EG, Poleszczuk J, et al. A proliferation saturation index to predict radiation response and personalize radiotherapy fractionation. *Radiat Oncol* 2015;10:1–8. [PubMed: 25567003]

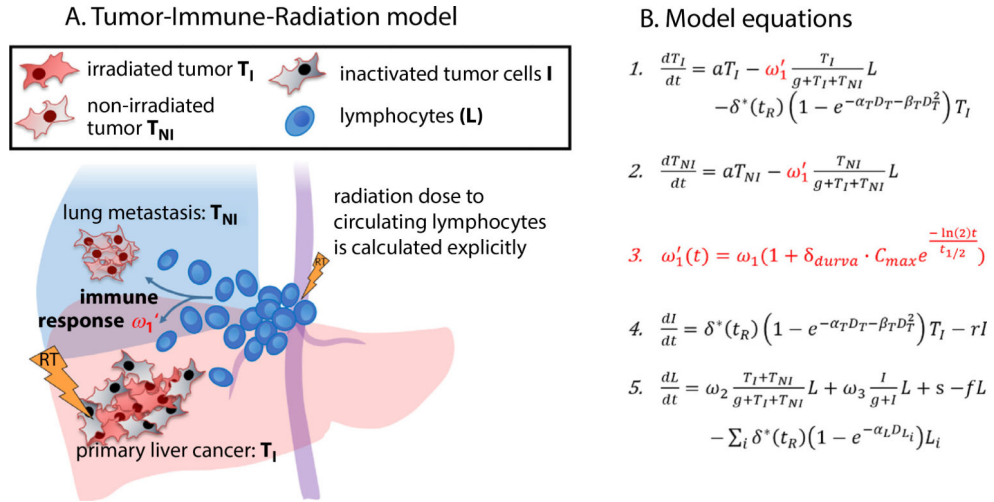


Fig. 1. Schematic overview over the model and the differential equations describing its dynamic behavior. Immune response (ω_1), induced by lymphocytes, exert a cytotoxic effect on both irradiated tumor and nonirradiated tumor cells. Immune response can be upregulated by the injection of Programmed Death-Ligand 1 (PD-L1) immune checkpoint inhibitors (durvalumab, red-marked new terms). Lightning symbolizes the radiation delivered to the primary liver cancer and circulating lymphocytes. Radiation dose to circulating lymphocyte is calculated explicitly using previously developed methods.¹¹

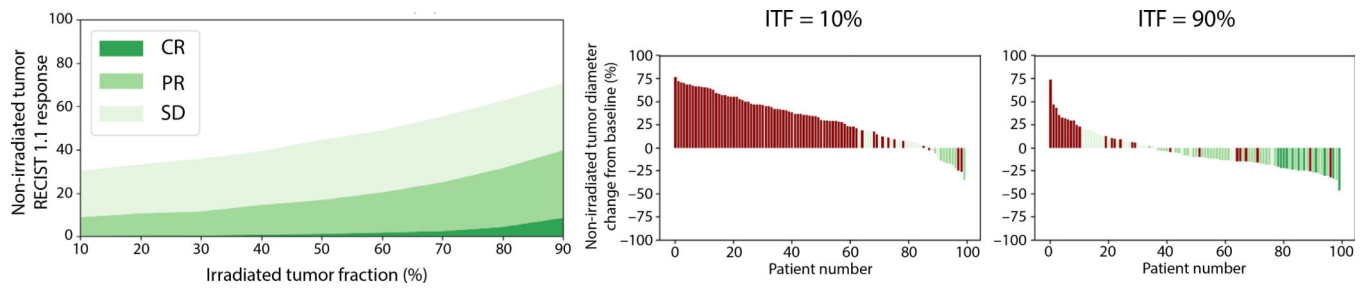


Fig. 2.

Predicted treatment outcome in nonirradiated lesions depending on irradiated tumor fraction.

Left: Predicted response in nonirradiated tumor as a function of irradiated tumor fraction).

Right: Tumor diameter change (in % change from baseline diameter at 6 months after the treatment start) of 2 simulated patient populations with 2 different irradiated tumor fractions (irradiated tumor fraction is 10% on left and 90% on right). Simulated immune checkpoint inhibitor-radiation therapy combination regimen: 8 Gy \times 3 radiation therapies delivered 2 weeks after the first immune checkpoint inhibitor dose. *Abbreviations:* CR = complete response; ITF = irradiated tumor fraction; PR = partial response; SD = stable disease.

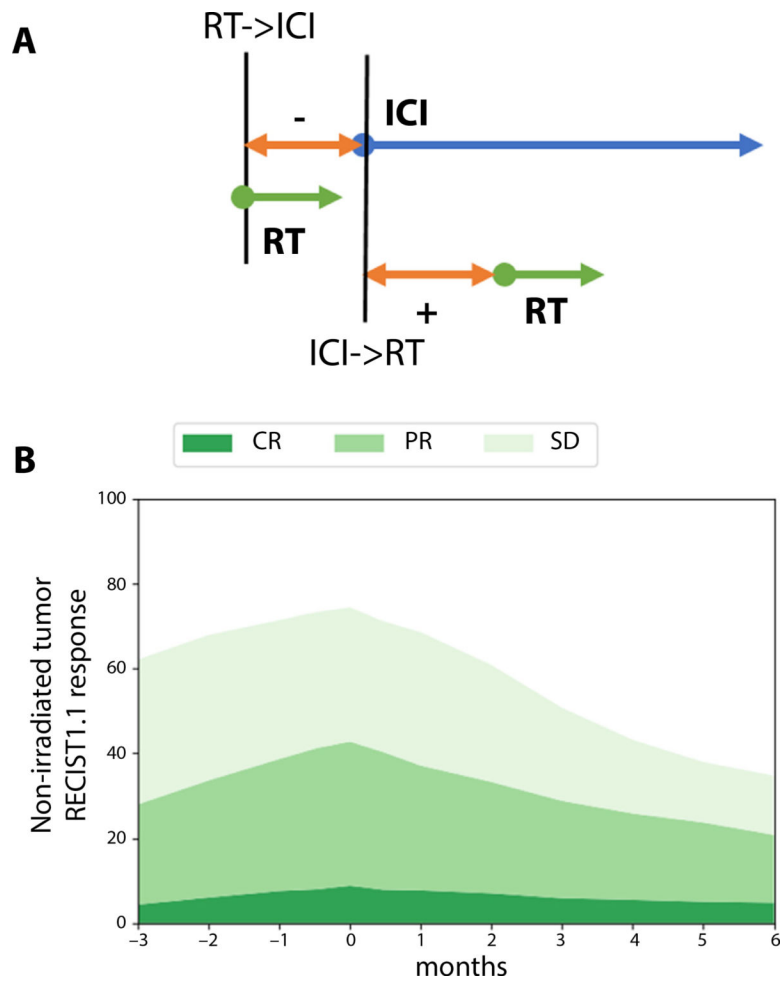


Fig. 3. Predicted treatment outcomes with different combination sequences. (A) Schematic providing the key for 3B: negative values on the time axis indicate RT started before immune checkpoint inhibitors, positive values indicate after immune checkpoint inhibitors. (B) Response rates as a function of radiation therapy start time for nonirradiated tumor. Radiation therapy is delivered as $8 \text{ Gy} \times 3$ to 90% of the tumor burden, that is, this case corresponds to the 90% irradiated tumor fraction case in Figure 1. *Abbreviations:* CR = complete response; ICI = immune checkpoint inhibitor; PR = partial response; RT = radiation therapy; SD = stable disease.

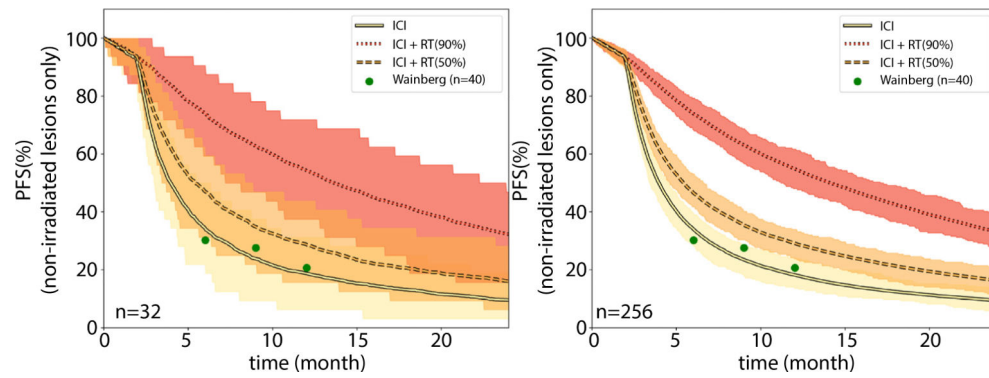


Fig. 4. Simulated trial outcomes for immune checkpoint inhibitor (ICI) monotherapy (solid line), ICI-radiation therapy (RT) with 50% of visible disease irradiated (dashed line), and ICI-RT with 90% of visible disease (dotted line) irradiated. RT consisted of $8\text{Gy} \times 3$, similar to a phase 2 trial.²³ The observed 6, 9, and 12 months of progression-free survival in the clinical trial for ICI monotherapy are shown as green circles. Results are shown for (A) 32 patients per arm and (B) 256 patients per arm. The shaded areas signify the expected 95% confidence intervals. The sharp fall-off step after 3 months stems from the assumption of follow-up scans every 3 months and so no progression events are observed before the first follow-up scan. *Abbreviations:* PFS = progression-free survival; ICI = immune checkpoint inhibitor; RT = radiation therapy.

Table 1

Summary of Model Parameters

Parameter	Description	Value	Treatment	Source	References
a	Tumor growth	0.01 d^{-1}	No treatment	Taken from literature	(11)
f	Lymphocyte decay rate	0.033 d^{-1}	No treatment	Taken from literature	(12)
Natural death	Unexpected natural death event rate not due to cancer progression	$4.2\%/mo$	No treatment	Taken from literature	(13)
α_T/β_T	Tumor – LQ cell kill	14.3 Gy	RT only	Taken from literature	(14)
r	Inactivated tumor cell decay rate	0.14 d^{-1}	RT only	Taken from literature	(15)
ω_1	Tumor-directed lymphocyte efficiency	0.119 d^{-1}	RT only	Fitted to local failure / distant metastasis in clinical trial NCT00976898	(9, 16)
ω_2, ω_3	Tumor/Inactivated tumor - lymphocyte recruitment constant	$0.003 \text{ d}^{-1}, 0.009 \text{ d}^{-1}$	RT only	Fitted to temporal lymphocyte counts in clinical trial NCT00976898	(9, 16)
g	Geometric saturation constant	7.330×10^{10}	RT only	Fitted to temporal lymphocyte counts in clinical trial NCT00976898	(9, 16)
s	Lymphocyte regeneration	$1.470 \times 10^8 \text{ d}^{-1}$	RT only	Fitted to temporal lymphocyte counts in clinical trial NCT00976898	(9, 16)
α_T	Tumor – LQ cell kill	Normally distributed ($\mu = 0.148, \sigma = 0.024$)	RT only	Fitted to local failure / distant metastasis in clinical trial NCT00976898	(9, 16)
α_L	Lymphocytes – LQ cell kill	0.737 Gy^{-1}	RT only	Fitted to temporal lymphocyte counts in clinical trial NCT00976898	(9, 16)
C_{max}	Maximum concentration	10 mg/kg	ICI only	Taken from literature	(17)
$t_{1/2}$	Half-life of immune checkpoint inhibitor (Durvalumab) in the body	21 days	ICI only	Taken from literature	(17)
δ_{durva}	Effectiveness of immune checkpoint inhibitor (Durvalumab)	Normally distributed ($\mu = 0.12, \sigma = 0.04$)	ICI only	Fitted to RECIST1.1 responses in clinical trial NCT01693562	(18)